SEMARAK ILMU PUBLISHING

Journal of Advanced Research in Fluid Mechanics and Thermal Sciences

Journal homepage:
https://semarakilmu.com.my/journals/index.php/fluid_mechanics_thermal_sciences/index
ISSN: 2289-7879

Grid Adaptive Technique for Simulation of Scramjet Intake-Isolator at Hypersonic Speeds

Juluru Sandeep[1,2,*], AVSS Kumara Swami Gupta[1]

[1] Department of Mechanical Engineering, JNTUH College of Engineering Hyderabad, India
[2] Department of Aero Engineering, School of Engineering and Technology, Sandip University, Nashik 422123, Maharashtra, India

ARTICLE INFO

Article history:
Received 28 May 2022
Received in revised form 23 October 2022
Accepted 3 November 2022
Available online 23 November 2022

Keywords:
Hypersonic intake; CFD; shock waves; Mach number

ABSTRACT

Hypersonic intake is one of the major components of Scramjet engine. It compresses the incoming hypersonic flow through a series of oblique shocks as the flow passes through intake-isolator section before entering the combustion chamber, which is essential for efficient combustion. The shocks generated inside in the intake interacts with boundary layer following shock boundary layer interaction and flow separation. The separated flow blocks the flow capture area such that engine expresses unstarting phenomenon. Understanding and mitigating such flow phenomenon is a challenging task. With respect to hypersonic speeds the experimental facilities are very limited. The only alternative to solve this problem is Computational Fluid Dynamics because of its capabilities. But validation of CFD results with analytical or experimental is the foremost prerequisite to chase computational analysis. Mostly at high speeds the precision of CFD results rest on the type of grid, number of elements and turbulence model used. So, in this paper, computational analysis of hypersonic intake is carried out through designed conditions to ensure the correct CFD process is used by varying number of elements in fluid domain by grid adaptive technique using ANSYS Fluent and satisfying Y^+ parameter. The domain is analysed with various turbulence models and among them SST has predicted all the flow characteristics of scramjet intake-isolator at hypersonic speeds like separation bubble, shock reattachment, cowl shock etc similar to experimental results with the help of grid adaptive technique. So, grid adaptive technique is also proposed for simulation of scramjet intake at off-design conditions.

1. Introduction

Scramjet is the only air-breathing engine to assist hypersonic speeds. But it has many complications and under research since 1950’s [1]. Scramjet takes hypersonic flow through intake and decelerates the flow to supersonic speeds with required pressure and temperature for combustion through a series of shocks. Majorly the complications are due to the compression part. So, the flow in intake-isolator section requires to be analyzed to understand: (1) shock wave-boundary layer interaction (SWBLI); (2) flow separation; (3) shock-shock interactions; and many

* *Corresponding author.*
E-mail address: julurusandeep@gmail.com

https://doi.org/10.37934/arfmts.101.1.7389

more. So, hypersonic intake efficiency is important for smooth performance of hypersonic vehicles. The intake has to be designed such that shock reflection makes flow parallel to free stream direction without any disturbance. The interaction of shocks with boundary layer should not lead to flow separation. The reflection of shocks should have maximum pressure recovery. These flow characteristics may lead to unstarting phenomenon of intake.

Analyzing above flow characteristics of hypersonic intake through experimental approach is difficult because of high enthalpy flow and temperature which may origin cooling and structural complications. So, the intake design for hypersonic speeds depends on occurrence of unstarting condition and to minimize it. Advanced research is going in both computational and experimental ways to recognize the reasons behind unstart of hypersonic.

Scramjet Intake-Isolator performance is classified according to its total pressure ratio and kinetic energy efficiency. Both performance indicators assume a quasi one-dimensional stream tube of flow through the intake, such as depicted in Figure 1. In Figure 1, Station 0 is the captured freestream prior to compression. Station 3 is downstream of the internal compression region and connects the intake-isolator with the combustor. Flow properties at Station 3 are used as input for all performance calculations.

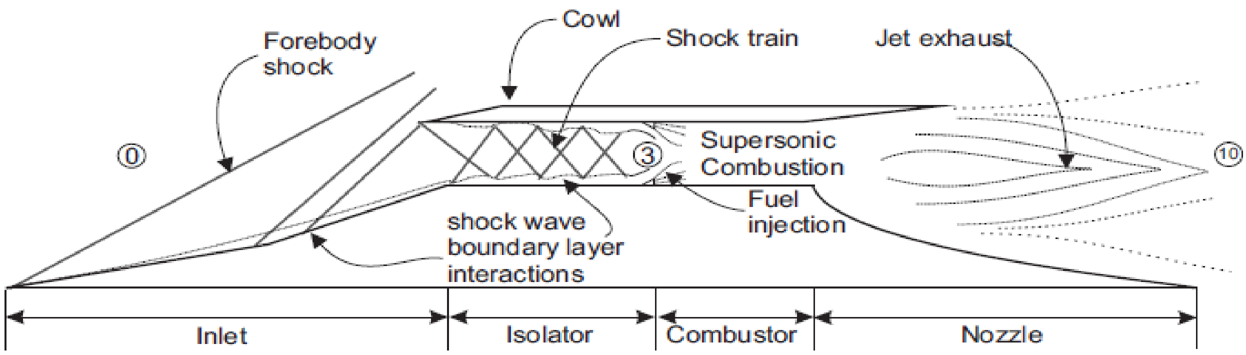

Fig. 1. Scramjet Engine [1]

2. Literature Review

Azam Che Idris *et al.,* validated CFD results with an optical luminescence flow diagnostics system developed using PSP to investigate the characteristics of a scramjet inlet-isolator [2]. Soumyajit Saha *et al.,* studied 2-D hypersonic intake characteristics with SST turbulence model using ANSYS Computational Fluid Dynamics software FLUENT. The CFD results are almost accurately matched with experimental results [3]. Azam Che Idris *et al.,* Suggested Y+ values less than 1 to simulate shock wave boundary layer interactions in hypersonic intake [4]. Senthil kumar *et al.,* have performed CFD simulations on SCRAMJET Inlet and noticed the direct effect of loss in total pressure recovery, inlet unsteadiness and flow distortion due to increase in cowl angle [5]. Janarthanam *et al.,* CFD results of three-dimensional flow in the dual mode scramjet intake-isolator are agreed with experimental results at Mach 4 using SST k-ω turbulence model [6]. Jonathan P. *et al.,* has noticed two turbulence models SA and SST could predict the unstarting condition of intake with flow separation bubbles [7].

Kbab Hakim *et al.,* used SST turbulence model in the simulation of Supersonic Nozzles to predict flow separation and thrust vectoring [8]. T. Nguyen *et al.,* computations had noticed achievement of Turbulence closure with two eddy-viscosity models (SST model and SST transition model) and a differential Reynolds-stress model with required corrections suitable to high-speed flows [9]. Christopher J. Roya, Frederick G. Blottner has recommended for the turbulence models (including newer models) are to be re-examined on the recent hypersonic experimental studies. Thus, any new turbulence model validation hard work must carefully evaluate the computational accuracy and model sensitivities [10]. Carter J. Waligura *et al.,* has investigated the effect of SA turbulence model in hypersonic flows with the help of grid adaption technique for a compression corner in hypersonic flows. The initial mesh is refined iteratively with reference to minimize the error evaluation of a fluid characteristic [11]. Aidan R *et al.,* performed computations on a cone in hypersonic flows to validated heat flux, static pressure, skin friction coefficient profiles and the flow contours using SA turbulence model with a coarse grid were accurate, but the results were departed from anticipation in heat flux, static pressure and Mach contours while refining the mesh [12]. Valerio Viti *et al.,* have used ANSYS Fluent CFD tool and predicted hypersonic flow physics and emphasized its capability of accuracy in analyzing the challenges of the hypersonic regime [13]. Jorge in his Master's thesis suggested SA and the k-ω Shear Stress Transport models for Hypersonic flow due to the strength of the SA model and the precision of the k- ω Shear Stress Transport model [14]. Krishna Zero *et al.,* had simulated hypersonic flow shock boundary-layer interaction with mesh adaptation in ANSYS Fluent successfully and suggested possibility of more accurate results with advanced reliability turbulence models [15]. Abhijeet Kumar recommended RANS methods with a SA turbulence model to capture the flow separation due to shock wave boundary layer interaction at Mach 5 in hypersonic intake [16]. Emad Qasem Hussein *et al.,* used Density based method in Ansys Fluent to simulate aerodynamic heating for a flying body at Hypersonic flows had comparatively good results with analytical results [17]. Delery. J. M, has pointed out that the present turbulence models are not enough to capture flow separation due to shock wave boundary layer interaction even though a fast improvement is seen in numerical methods. He elucidated about the importance of designing new transport equation models to perform more efficiently predicting complex flow structures or phenomenon like shock wave boundary layer interactions [18]. Thangadurai Murugan *et al.,* have performed CFD analysis on scramjet engine using SST turbulence model in ANSYS CFX. They have predicted a strong separation bubble on the bodyside wall in the internal compression region [19]. Julian D. Cecil also used ANSYS Fluent solving unsteady Reynolds-Averaged compressible Navier-Stokes equations with SA turbulence model for analyzing hypersonic flow over a cone. But the results are having significant error when compared to experimental at the leeward meridian of the cone. So, they concluded a need of change in the grid and also the turbulence models, it is likely to improve accuracy of the computations [20]. Saha in his computations stated the difference of inviscid and viscous simulation to understand starting/unstarting behavior of hypersonic intakes using ANSYS Fluent by solving Euler and Reynolds Average Navier stokes equations [21]. Arup kumar Biswas *et al.,* has performed grid dependency study for various number of grid elements with respect to temperature profile and found decrease in computation time [22].

3. Problem Definition

A widespread work has been studied on Hypersonic intakes using CFD as detailed in Literature review. But the impact of grid methods, turbulence model and computation time on the results is not studied promptly. The studies carried on grid independence were majorly on variable mesh and mesh is refined without adapting solution of coarse mesh. With this mode of grid generation increases number of elements and computation time. Even most of the research work used second order spatial discretization. So, in the present paper CFD simulations of hypersonic intake isolator are performed and validate with experimental results. Geometry and boundary conditions for the simulations is referred from Iridis *et al.,* [2] as shown in Figure 2.

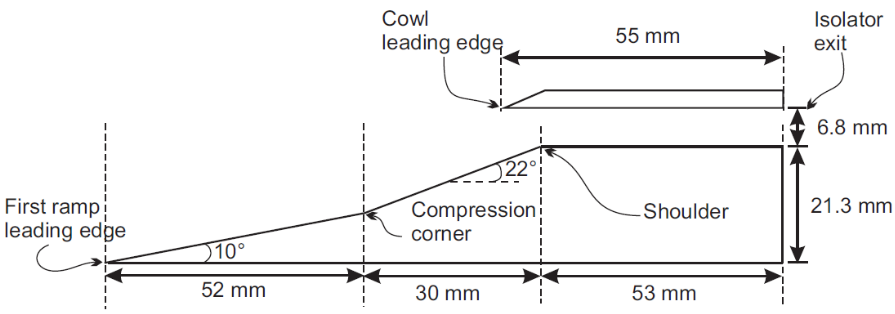

Fig. 2. Hypersonic intake model [2]

4. Analytical Results

The flow in the intake at hypersonic speeds come across with a series of multiple shocks and the output of these shocks can be calculated analytically by following the oblique shock relations from Modern compressible flow Anderson [23] with respect to Figure 3.

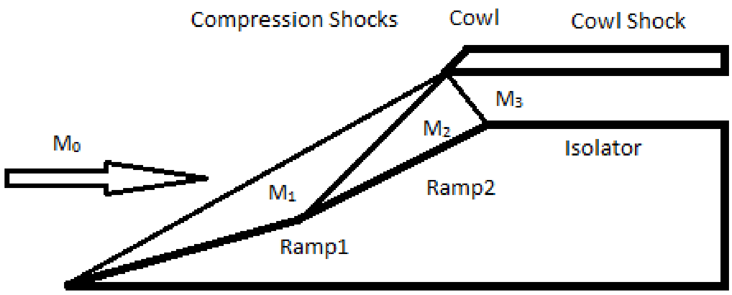

Fig. 3. Series of oblique shocks in intake-isolator of Scramjet engine [2]

Analytically the following oblique shock relations are used.

$$tan\theta = 2cot\beta\left[\frac{M_0^2 sin^2\beta - 1}{M^2_{0\,(\gamma+cos^2\beta)+2}}\right] \quad (1)$$

The normal component of Mach number across oblique shock is

$$M_{n0} = M_0 \sin\beta \quad (2)$$

From Normal Shock Tables M_{n1} is obtained. The Mach number behind the shock is given by

$$M_1 = \frac{M_{n1}}{Sin\ (\beta - \Theta)} \quad (3)$$

Pressure ratio across shock is given by

$$\frac{P_1}{P_0} = 1 + \frac{2\gamma}{\gamma+1}(M_{n0}^2 - 1) \quad (4)$$

Density ratio

$$\frac{\rho_1}{\rho_0} = \frac{(\gamma + 1)M_{n0}^2}{(\gamma - 1)M_{n0}^2 + 2} \tag{5}$$

Temperature ratio

$$\frac{T_1}{T_0} = \frac{P_1}{P_0}\frac{\rho_0}{\rho_1} \tag{6}$$

Total Pressure ratio across shock waves is given by

$$\frac{P_{t1}}{P_{t0}} = \frac{P_0}{P_{t0}}\frac{P_1}{P_0}\frac{P_{t1}}{P_1} \tag{7}$$

The change in flow properties across series of reflected shock waves from the intake isolator are calculated using above relations as per the series of reflected shocks shown in Figure 3 and tabulated in Table 1. From the geometry of hypersonic intake isolator of Figure 2, $\theta = 10^0$ and then from Eq. (1) for M_0=5 and angle $\theta = 10^0$ the shock wave angle β is 19.37^0. Using Eq. (2) we get M_{n0} =1.658. Then from Normal shock tables M_{n1}= 0.65 and from Eq. (3) we get M_1 = 4. Similarly, Eqs. (4)-(7) gives static pressure, density, temperature and total pressure ratios across shocks.

The same procedure is followed for all the shocks to know the flow properties at the inlet of isolator and tabulated in Table 1.

Table 1
Flow properties across shock waves

M_0	β_0	M_1	$\frac{P_1}{P_0}$	$\frac{\rho_1}{\rho_0}$	$\frac{T_1}{T_0}$	β_1	M_2	$\frac{P_2}{P_1}$	$\frac{\rho_2}{\rho_1}$	$\frac{T_2}{T_1}$	β_2	M_3	$\frac{P_3}{P_2}$	$\frac{\rho_3}{\rho_2}$	$\frac{T_3}{T_2}$
5	19.44		3.04	2.12	1.43	24	3.14	2.95	2.08	1.41	39	1.97	4.4	2.64	1.67

From the above results the pressure ratio across shock waves from two ramps is same, satisfying one of the design criteria of mixed compression inlet for Scramjet engines. The cowl angle has to be changed to satisfy the condition of Mach number at entrance of isolator should not be less than half of the freestream Mach number. Total pressure recovery is also around 55% which defines the best design of intake for Scramjet. But in the off-design condition same strength of shocks couldn't be generated by intake at higher Mach numbers 6 and 7. In real flow due to viscous effects the performance of intake may change. So, in the present analysis inviscid relation results tabulated in Table1 are used to compare CFD results to verify shock pattern and experimental results re used to compare flow characteristics.

5. Computational Methodology

The first step in the computational fluid dynamics is to identify fluid domain to be solve and generate grid for solving fluid flow governing equations. N. Vinayaka *et al.,* used ICEM CFD to generate structured grid to simulate shock waves for a high altitude transonic supercritical aerofoil [24]. So, the present geometry is also used ICEM CFD for designing and meshing as shown in Figure 4 and Figure 5.

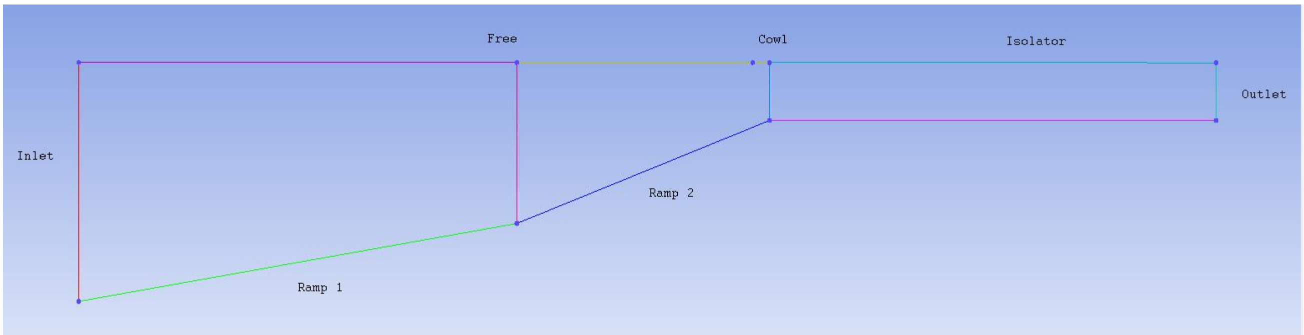

Fig. 4. Hypersonic Intake design in ICEM CFD

The next step is dividing fluid domain into small volumes or cells is known as grid, it is carried out in ANSYS ICEM CFD tool. Grid is a small control volume of the whole flow domain which is solved by all the governing equations based on which the results of flow variations can be obtained. The mesh geometry is given below in Figure 5. The grid is generated based on thickness of shock *i.e.,* 10^{-5} cm which is 0.001 mm. So, initially in the edge mesh law 4 times the length of edge is taken as number of nodes for all the edges. Such that around 60,480 cells are obtained as shown in figure below.

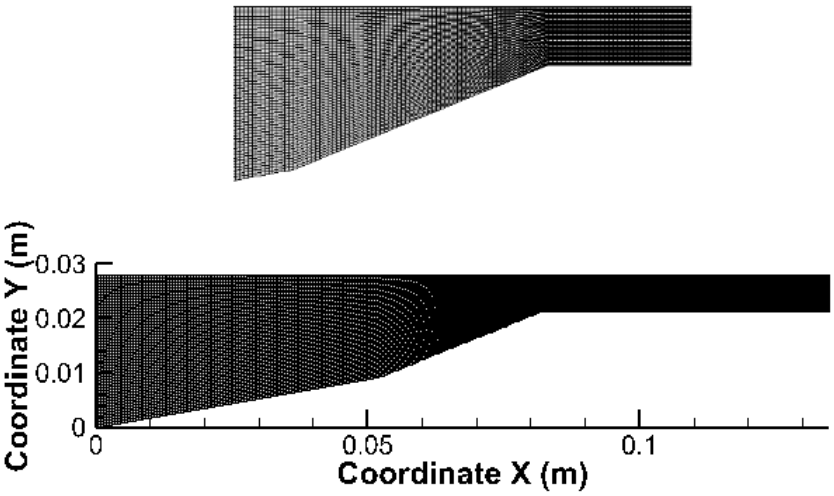

Fig. 5. Fluid domain and mesh quality with structured grid

In Computational Fluid Dynamic the next step is to solve fluid flow governing equations [25]. So, in the present work density-based solver is used for solving RANS equations by various turbulence models with 2nd order discretization. The suitable equations governing the high-speed flow may be written as

Continuity equation

$$\frac{\partial \rho}{\partial t} + \frac{\partial \rho}{\partial x_k}(\rho u_k) = 0 \tag{8}$$

k = 1, 2, 3

Momentum equation

$$\frac{\partial}{\partial t}(\rho u_i) + \frac{\partial \rho}{\partial x_k}(\rho u_i u_k) + \frac{\partial P}{\partial x_i} = \frac{\partial(\tau_{ik})}{\partial x_i} \tag{9}$$

i, k = 1, 2, 3

Energy equation

$$\frac{\partial}{\partial t}(\rho E) + \frac{\partial}{\partial x_k}(\rho u_k H) = -\frac{\partial}{\partial x_i}\left(u_j \tau_{jk}\right) + \frac{\partial(q_k)}{\partial x_i} \tag{10}$$

j, k=1, 2, 3

where ρ is density, u_i is velocity, P is pressure, E is total energy and H is enthalpy. Turbulent shear stress is

$$\tau_{jk} = \mu\left[\frac{\partial u_i}{\partial x_k} + \frac{\partial u_k}{\partial x_i}\right] \tag{11}$$

The present simulations are solved in ANSYS FLUENT in density-based solver. Stability is ensured by setting the Courant–Friedrichs–Levy (CFL) number to 0.5 initially and gradually increasing it by the same value every 1,000 iterations. The computational domain is bounded by a pressure far-field, constant temperature walls and pressure outlet as shown in Figure 4.

5.1 Boundary Conditions

The above fluid domain is solved for the following boundary conditions taken from the experimental paper [2] and conditions belong to an altitude of 30km and are as shown in Table 2 to understand flow physics.

Table 2
Boundary Conditions

S. No	Location	Boundary	Value
1	Inlet	Pressure farfield	Static pressure = 1228 Pa Mach No=5
2	Outlet	Pressure outlet	Pressure=0 (Pa)
3	Ramp,Cowl, Isolator	Wall	No slip
5	Free	Wall	No slip with specified shear zero

ANSYS Fluent solver is used for post processing of results such as distribution of Mach contour, Pressure, Density and Temperature of CFD result are shown in figures below.

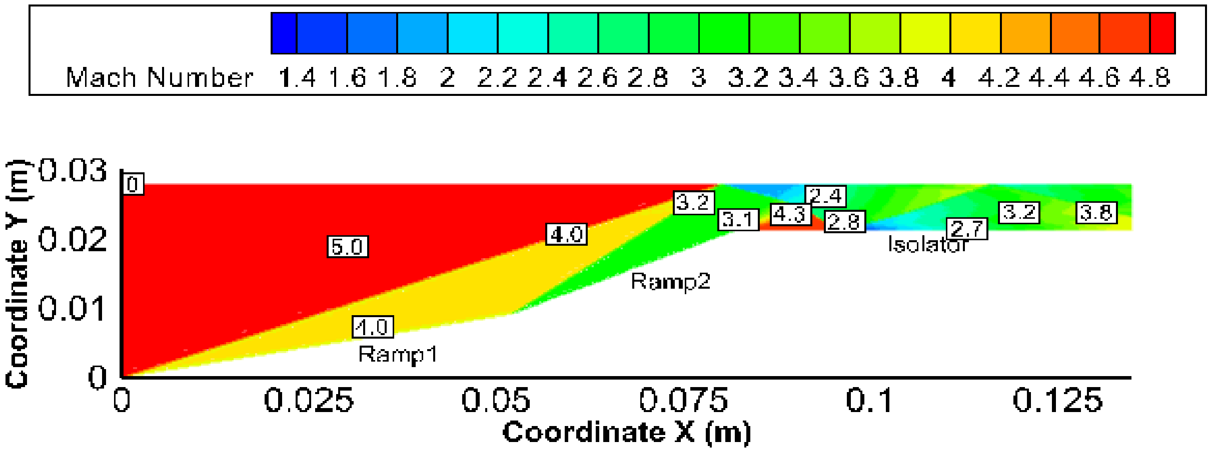

Fig. 6. Mach contour of hypersonic intake at M=5 for initial grid

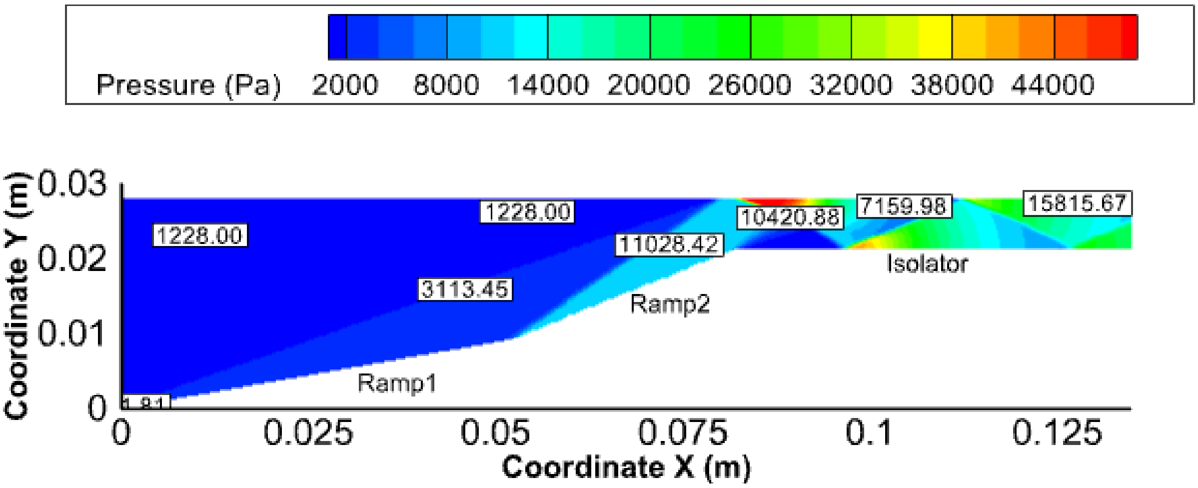

Fig. 7. Pressure contour of hypersonic intake at M=5 for initial grid

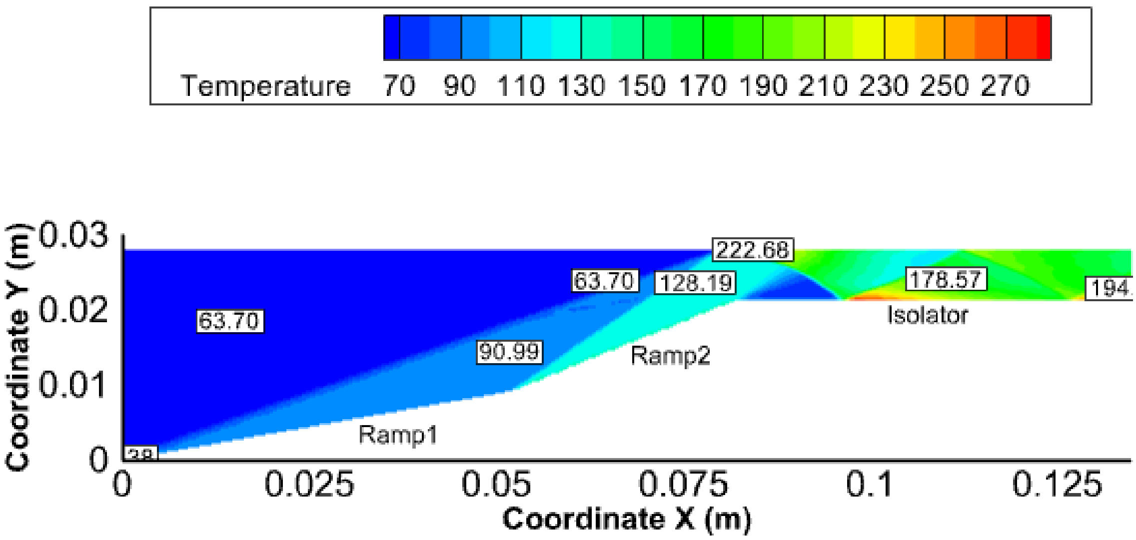

Fig. 8. Temperature contour of hypersonic intake at M=5 for initial grid

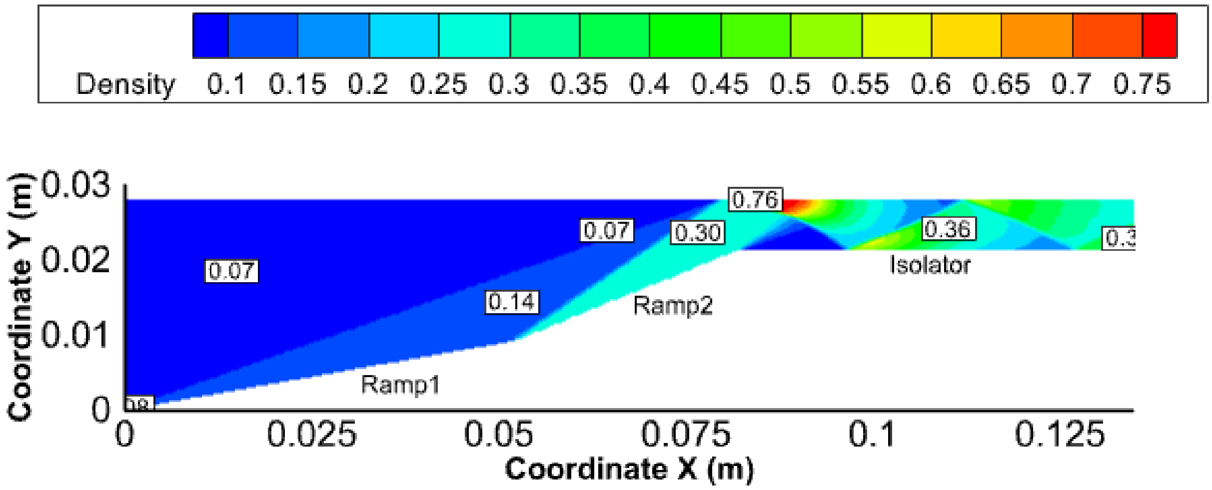

Fig. 9. Density contour of hypersonic intake at M=5 for initial grid

From the above CFD results the shock reflections have been captured and the variation in flow properties are compared with analytical results as shown in Table 3.

Table 3
Comparison of CFD results with Analytical results

Results	M_0	M_1	$\frac{P_1}{P_0}$	$\frac{\rho_1}{\rho_0}$	$\frac{T_1}{T_0}$	M_2	$\frac{P_2}{P_1}$	$\frac{\rho_2}{\rho_1}$	$\frac{T_2}{T_1}$	M_3	$\frac{P_3}{P_2}$	$\frac{\rho_3}{\rho_2}$	$\frac{T_3}{T_2}$
Analytical	5	4	3.04	2.12	1.43	3.14	2.95	2.08	1.41	1.97	4.4	2.64	1.67
CFD	5	4	2.54	2	1.4	3.15	3.54	2.14	1.4	2.4	4	2.53	1.74

6. Grid Independence Study and Validation

Grid plays a dominant role in attaining accurate results but simultaneously it effects computation time. As capturing shock waves is most important in hypersonic flows, grid is changed to capture exact shocks. Increasing number of cells for a given domain uniformly obviously increases computation time but the size and number of cells play a major role in getting accurate results especially for hypersonic flows. So, refinement of the generated grid is needed to capture flow physics and to validate results. In refinement of grid, grid adaption technique using pressure gradient for inviscid simulations and y+ criteria for viscous simulations are used. CFD results of initial grid from Figures 6 to Figure 9 is not matching with analytical results as shown in Table 3. So, refinement of grid is necessary to validate grid. Grid adaption technique generates new cells in the region, which has pressure gradient. From Figure 3 the shock region is identified then refinement of grid is adapted to only such regions. The grid adaption technique accommodates dense grid near shock regions as shown in Figure 10 and Figure 11.

As mentioned in Table 4 the number of elements for various grids and its results for designed condition are compared in Figure 14 with pressure distribution along ramp and isolator bottom wall which defines the shock strength. Among them grid3 has given good results with exact shock reflections, shock on lip condition and flow properties are also matching with Table 2 results.

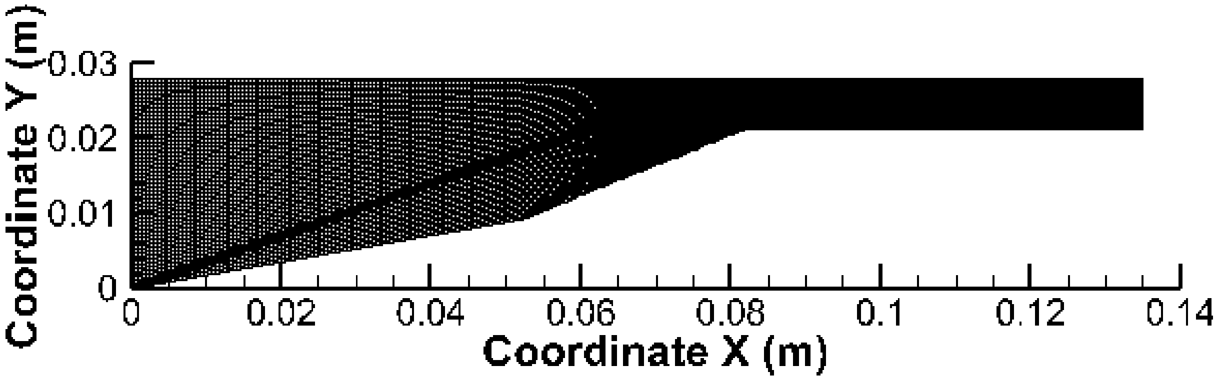

Fig. 10. Refined Grid due to grid adaption technique

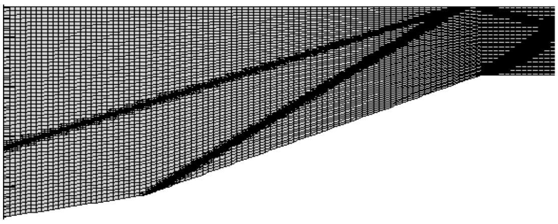

Fig. 11. Zoomed view of Grid at shock regions

Table 4
Types of Grid

S. No	Case	Number of elements	Time taken in seconds for 100 iterations
1	Grid 1	60480	578
2	Grid 2	178554	1452
3	Grid 3	298749	1982

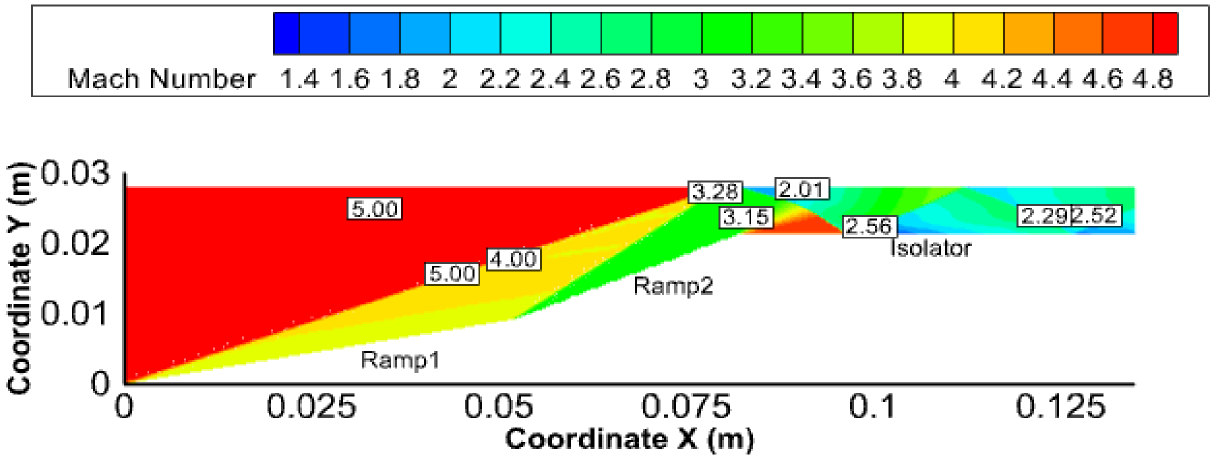

Fig. 12. Mach contour of hypersonic intake at M=5 for grid 2

Out of all the grids analyzed, grid 3 has given correct variation of Mach number along the multiple shocks with M_0=5, M_1=4, M_2=3.14 and M_3=1.9 compared to grid1 and grid2 Mach contours as shown in Figure13.

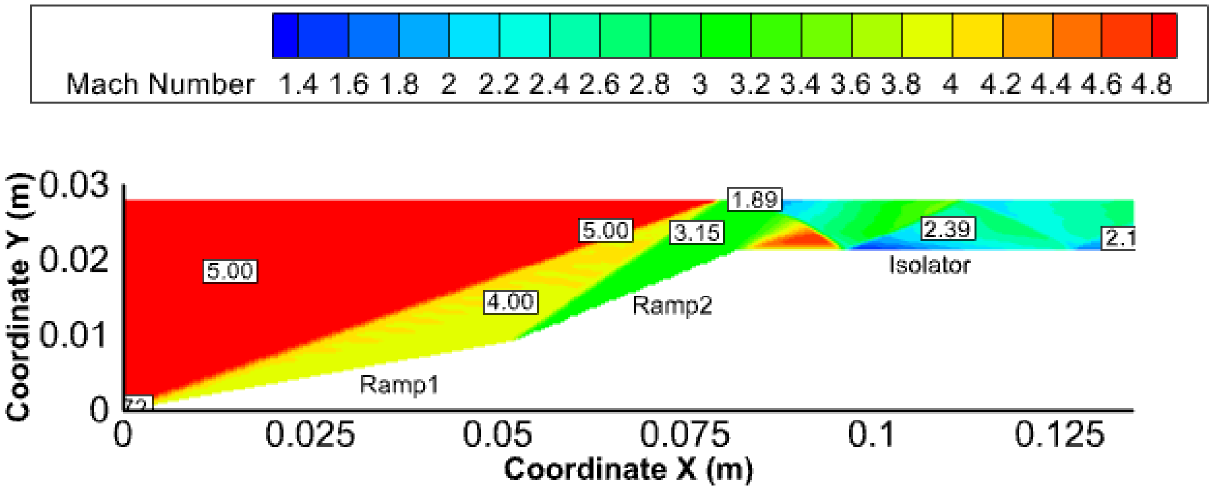

Fig. 13. Mach contour of hypersonic intake at M=5 for grid 3

The CFD solution has studied grid independence of the domain and had optimised number of cells required based on Mach contour and Pressure contour as shown in Figure 14. These CFD solutions are validated with analytical results with inviscid oblique shock relations but not with experimental results which has viscous effects. In hypersonic flows along with shock reflections, boundary layer also plays an important in predicting starting problems of intake. So, refinement of grid is required for capturing boundary layer and is estimated based on y+ value along the walls like ramp, cowl and isolator. With basic designed grid the Y^+ value is 178.6. But to capture boundary layer it should be less than 1. So, the minimum element Δs is 0.008 mm calculated as per the following formulae taken from flat plate boundary layer theory of Fluid Mechanics by White [26].

Element size $\Delta s = \frac{y^+\mu}{U_{fric}\rho}$ (12)

Frictional velocity $U_f = \sqrt{\frac{\tau_w}{\rho}}$ (13)

Shear stress at wall $\tau_W = \frac{C_f \rho U_\infty^2}{2}$ (14)

Coefficient of friction $C_f = \frac{0.026}{Re_x^{1/7}}$ (15)

Reynolds number $Re_x = \frac{\rho U_\infty L}{\mu}$ (16)

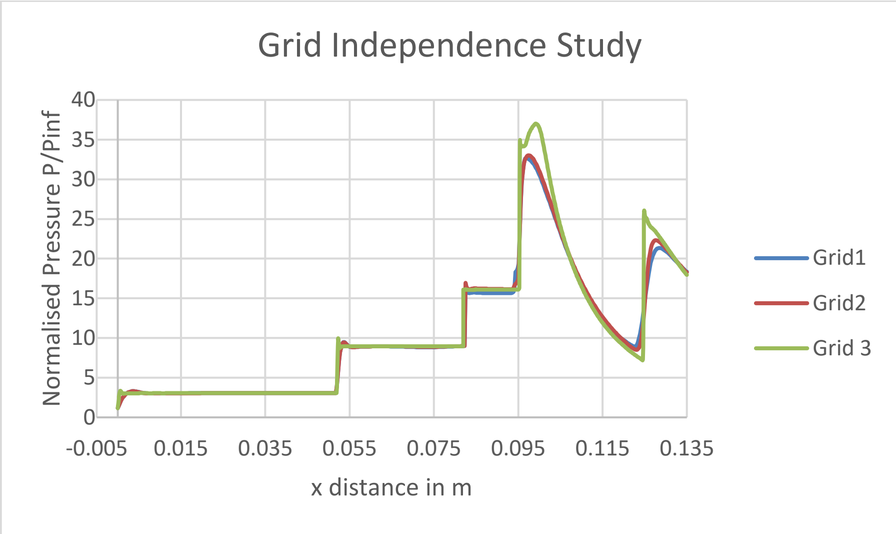

Fig. 14. Pressure distribution along ramp and isolator bottom wall for grid independence study

Applying refinement of grid with respect to achieve Y^+ value less than 1 the number of cells along walls of the domain has increased as shown in Figure 15. The total number of cells attained are 394562.

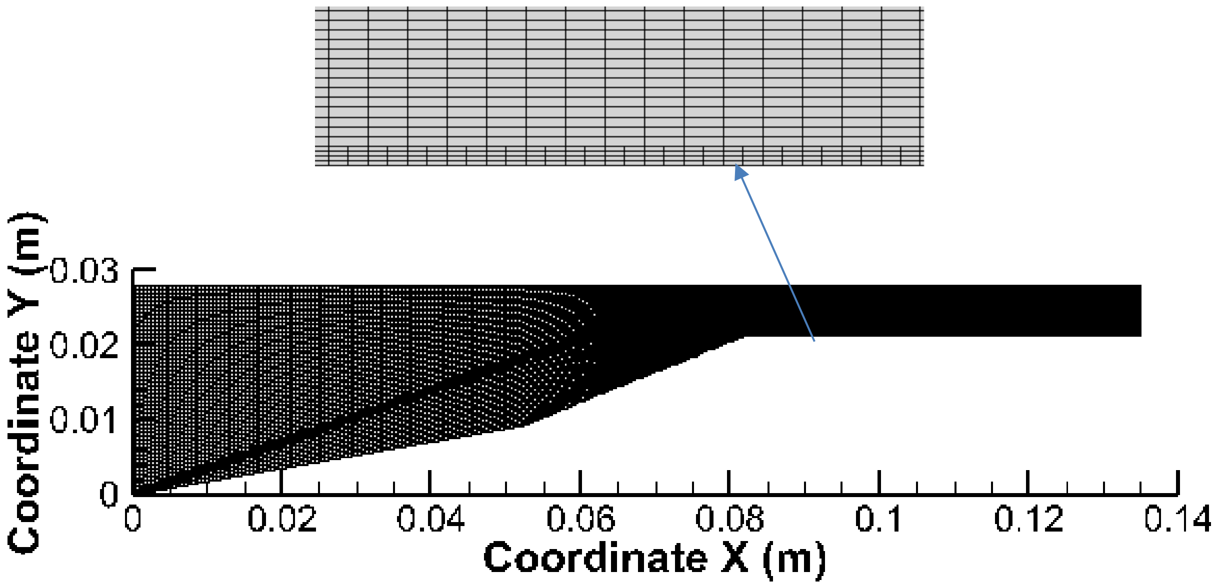

Fig. 15. Refined grid due to Y^+

7. Serial and Parallel Processing

In computational analysis, processor of the computer plays key role in achieving the accurate results within less time. Since computation time depends on the number of elements in domain and the complexity of problem. In the present work, the flow speed is hypersonic which leads to formation of various flow phenomenon like shock waves, boundary layers, flow separation, vortices. So, the number of cells required for present problem depends mainly on y^+ value and shock wave. From the previous section 394562 number of cells are optimised for the present problem. The computation time taken for it in a single processor is around 2124 seconds. The improvement in computational architecture to solve complex problems using parallel processing reduced time for computation by increasing the number of processors for single problem. In serial processing a single processor simulates the complete fluid domain but in parallel processing multiple number of processors are assigned and fluid domain is partitioned into equal number of processors. Table 4 illustrates the computation time for 394562 number of cells for 100 iterations. So, the research work is solved in an INTEL CORE i5 CPU with 8GB RAM and 4 processors.

Table 4
Computation Time for 100 iterations using Parallel Processors

Number of processors	Computation time (sec)
1	2124
2	1450
3	847
4	521

8. Impact of Turbulence Models

In the above cases inviscid and viscous simulations are carried to optimise the grid and computational power for the given fluid domain. But the real flow is of viscous need an efficient turbulence model to capture hypersonic flow physics. In CFD, turbulence model for the simulations of hypersonic flows in scramjet engine is also one of the critical parameters in predicting the induced flow separations due to shock/boundary-layer interactions. The main aim of the present section remains to understand the impact of turbulence models in analyzing the hypersonic flow-field through a scramjet intake. The results are used to suggest a turbulence model for the off design simulations.

It is an unfortunate fact that no single turbulence model is universally accepted as being superior for all classes of problems. The choice of turbulence model will depend on considerations such as the physics encompassed in the flow, the established practice for a specific class of problem, the level of accuracy required, the available computational resources, and the amount of time available for the simulation. To make the most appropriate choice of model for hypersonic flow application, one need to understand the capabilities and limitations of the various options. In the present analysis SA – one equation, k-ε – two equation and SST – four equation turbulence models are used to get the exact flow pattern matching with experimental results [2].

SA turbulence model couldn’t capture flow separation and k epsilon model couldn’t capture cowl tip separation and reattachment shock downstream of flow separation as shown in Figures 16 and Figure 17. Thus, SST model is used in further simulations. From the above results the both turbulence models results are over predicted related to incident shock strength from two ramps.

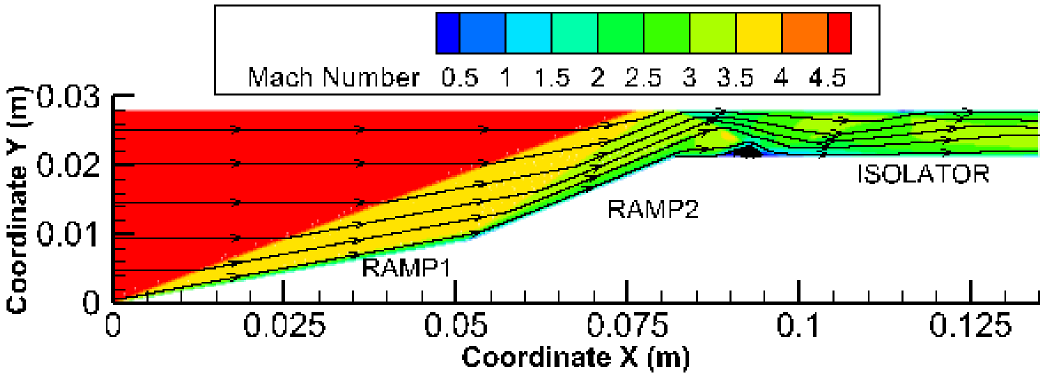

Fig. 16. Mach contour of Hypersonic intake for SA turbulence model

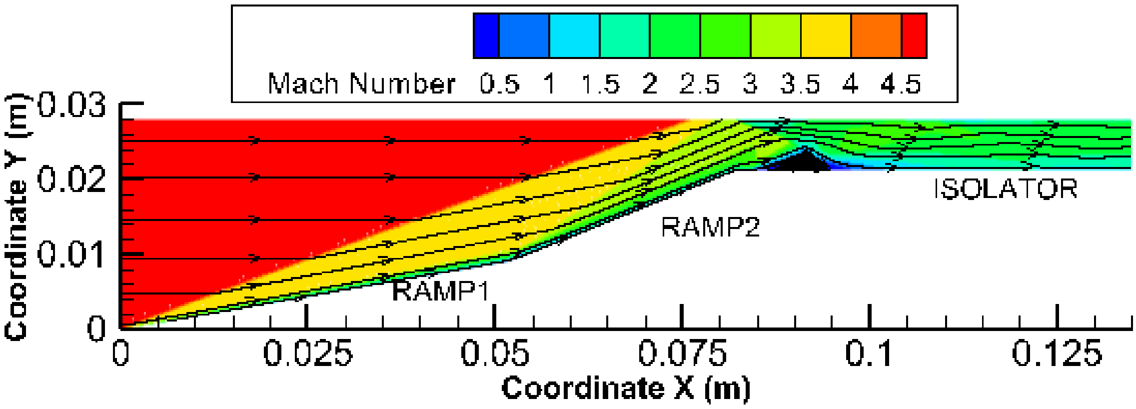

Fig. 17. Mach contour of Hypersonic intake for k epsilon turbulence model

Figures below gives the impact of turbulence models and grid adaptive technique in predicting hypersonic flow pattern with respect to experimental results [2]. Among three models used SST turbulence model gives accurate shock pattern, flow separation as shown in Figure 18.

From the Mach contour it is noticed, there are three noticeable flow characteristic changes are

i. the flow separation at the shoulder due to cowl shock boundary layer interaction;
ii. multiple reflection of shocks and separation points;
iii. the re-attachment shock from the third separation bubble

The streamline pattern from the inlet through ramps to inside of the isolator section shows the change in flow behaviour due to shock waves and boundary layer. Meanwhile the wave attained inside the isolator due to cowl tip shock impingement downstream of the shoulder shows the distortion level in the flow. Flow phenomenon is smooth in designed condition and takes shock on lip condition as per above results without disturbances. The same CFD model can be used in off design conditions at Mach 6, 7 and 4.

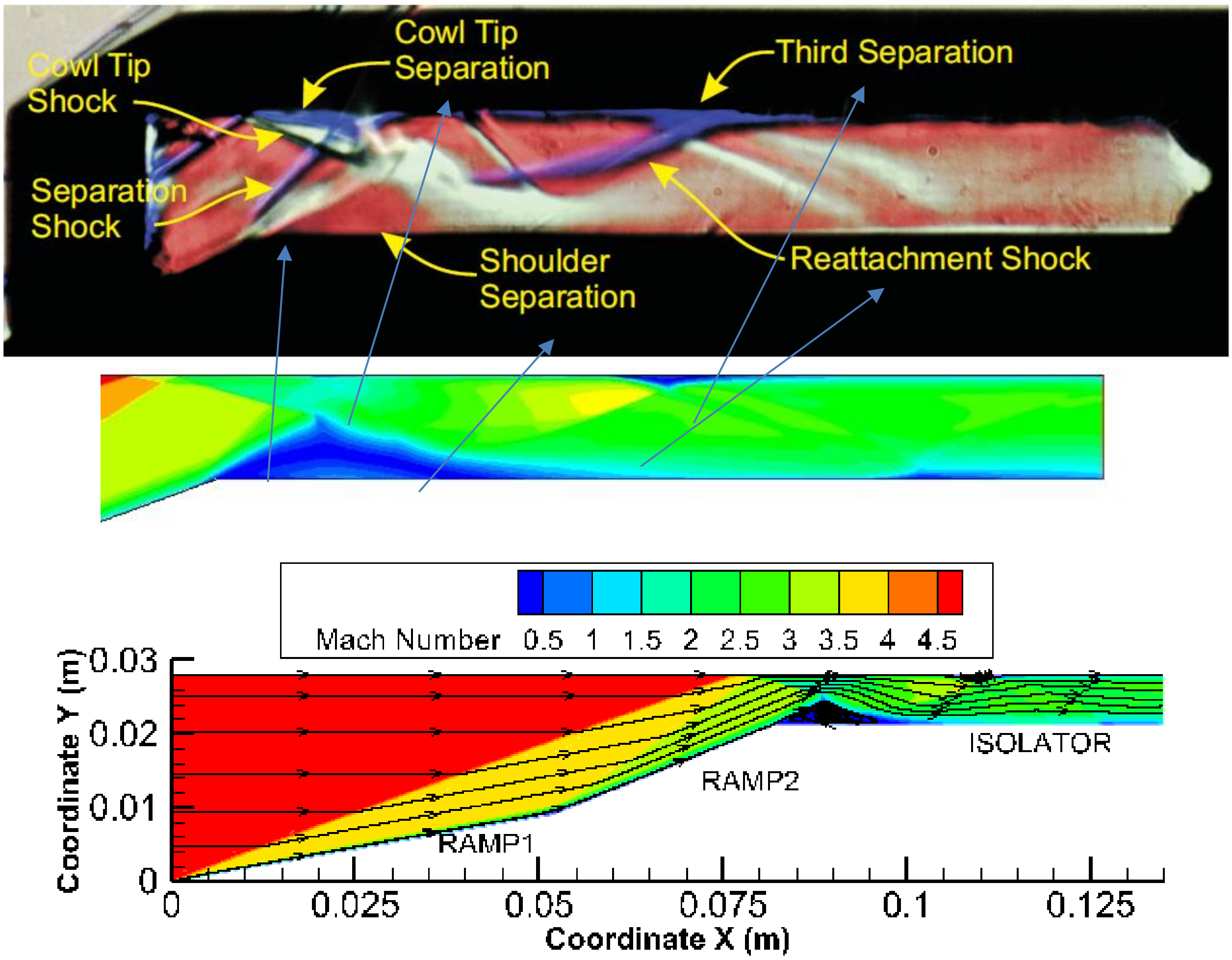

Fig. 18. Comparison of Mach contour of Hypersonic intake for SST turbulence model with experimental flow pattern [2]

9. Conclusions

In the present paper the main focus is to define a computational model to simulate the hypersonic flow through hypersonic intake isolator. ANSYS Fluent is used for simulation and the present analysis carried out by various grids and turbulence models out of which grid adaption technique and SST turbulence model is suitable for hypersonic intake in predicting hypersonic flow characteristics like shock on lip condition, shock boundary layer interaction and flow separation which are validated with experimental results. Mach number, Pressure, Temperature and density ratios across oblique shock wave of CFD results are exactly matching with analytical results. So, the future scope of the present work is the proposed grid adaptive technique can be used for further off design simulations to understand hypersonic intake performance with exact shock impingements and flow separations. It can also be applied for all types of shock problems in supersonic and hypersonic flows.

Acknowledgments
The author is very much thankful to the Department of Aero Engineering, School of Engineering and Technology and Management of Sandip University for providing facilities to carryout CFD simulations and in writing paper.

References

[1] Fry, Ronald S. "A century of ramjet propulsion technology evolution." *Journal of propulsion and power* 20, no. 1 (2004): 27-58. https://doi.org/10.2514/1.9178

[2] Idris, Azam Che, Mohd Rashdan Saad, Hossein Zare-Behtash, and Konstantinos Kontis. "Luminescent measurement systems for the investigation of a scramjet inlet-isolator." *Sensors* 14, no. 4 (2014): 6606-6632. https://doi.org/10.3390/s140406606

[3] Saha, Soumyajit, and Debasis Chakraborty. "Hypersonic intake starting characteristics–A CFD Validation study." *Defence Science Journal* 62, no. 3 (2012): 147-152. https://doi.org/10.14429/dsj.62.1340

[4] Idris, Azam Che, Mohd Rashdan Saad, and Konstantinos Kontis. "Potential of Micro-Vortex Generators in Enhancing the Quality of Flow in a Hypersonic Inlet-Isolator." *Journal of Advanced Research in Fluid Mechanics and Thermal Sciences* 77, no. 1 (2021): 1-10. https://doi.org/10.37934/arfmts.77.1.110

[5] Janarthanam, S., and V. Babu. "Numerical simulations of the flow through the inlet and isolator of a mach 4 dual mode scramjet." *The Aeronautical Journal* 116, no. 1182 (2012): 833-846. https://doi.org/10.1017/S0001924000007302

[6] INTAKES, PERFORMANCE OF SCRAMJET AIR. "Effect of Cowl angle in the performance of scramjet air intakes." *Technology* 8, no. 11 (2017): 899-909.

[7] Reardon, Jonathan P., Joseph A. Schetz, and Kevin Todd Lowe. "Computational Analysis of Unstart in Variable-Geometry Inlet." *Journal of Propulsion and Power* 37, no. 4 (2021): 564-576. https://doi.org/10.2514/1.B38214

[8] Hakim, Kbab, Hamitouche Toufik, and Y. Mouloudj. "Study and Simulation of the Thrust Vectoring in Supersonic Nozzles." *Journal of Advanced Research in Fluid Mechanics and Thermal Sciences* 93, no. 1 (2022): 13-24. https://doi.org/10.37934/arfmts.93.1.1324

[9] Nguyen, Tue, Gero Schieffer, Christian Fischer, Herbert Olivier, Marek Behr, and Birgit Reinartz. "Details of turbulence modeling in numerical simulations of scramjet intake." In *27th Congress of International Council of the Aeronautical Sciences (ICAS), Nice, France*, (2010): 19-24.

[10] Roy, Christopher J., and Frederick G. Blottner. "Review and assessment of turbulence models for hypersonic flows." *Progress in Aerospace Sciences* 42, no. 7-8 (2006): 469-530. https://doi.org/10.1016/j.paerosci.2006.12.002

[11] Waligura, Carter J., Benjamin L. Couchman, Marshall C. Galbraith, Steven R. Allmaras, and Wesley L. Harris. "Investigation of Spalart-Allmaras Turbulence Model Modifications for Hypersonic Flows Utilizing Output-Based Grid Adaptation." In *AIAA SCITECH 2022 Forum*, (2022): 0587. https://doi.org/10.2514/6.2022-0587

[12] Viti, Valerio, Bruce Crawford, Carlo Arguinzoni, Vinod Rao, and Laith Zori. "Numerical validation of four canonical hypersonic vehicles and test-cases." In *AIAA AVIATION 2020 FORUM*, (2020): 2723. https://doi.org/10.2514/6.2020-2723

[13] Murphy, Aidan R., and Ramesh K. Agarwal. "Computational Analysis of the HIFiRE-1 Hypersonic Test Model in ANSYS Fluent." In *AIAA AVIATION 2022 Forum*, (2022): 4047. https://doi.org/10.2514/6.2022-4047

[14] Bretzke, Jorge-Valentino Kurose. "Comparison of Reynolds-averaged Navier-Stokes turbulence models for simulating boundary layers in hypersonic flows.". Missouri University of Science and Technology, (2020).

[15] Zore, Krishna, Isik Ozcer, Luke Munholand, and John Stokes. "ANSYS CFD Simulations of Supersonic and Hypersonic Flows."

[16] Kumar, Abhijeet, and Ben Thornber. "RANS modelling of shock-wave boundary layer interaction in a mixed compression axisymmetric hypersonic intake." In *Applied Mechanics and Materials*, vol. 846 (2016): 61-66. https://doi.org/10.4028/www.scientific.net/AMM.846.61

[17] Hussein, Emad Qasem, Farhan Lafta Rashid, and Haider Nadhom Azziz. "Aerodynamic heating distribution for temperature prediction of fast flying body nose using CFD." *Journal of Advanced Research in Fluid Mechanics and Thermal Sciences* 64, no. 2 (2019): 183-195.

[18] Delery, J., and J. G. Marvin. "Turbulent shock-wave/boundary layer interaction." *AGARDograph 280* (1986).

[19] Murugan, Thangadurai, Sudipta De, and V. Thiagarajan. "Validation of three-dimensional simulation of Flow through Hypersonic air-breathing engine." *Defence Science Journal* 65, no. 4 (2015): 272-278. https://doi.org/10.14429/dsj.65.6979

[20] Cecil, Julian. "Validation of CFD Simulations for Hypersonic Flow Over a Yawed Cone." *Master of Aerospace Engineering Washington University in St. Louis* (2018).

[21] Saha, Soumyajit, and Debasis Chakraborty. "Role of viscosity in hypersonic intake starting phenomenon." *J Aerosp Sci Technol* 69, no. 1 (2017): 18-24.

[22] Biswas, Arup Kumar, Wasu Suksuwan, Khamphe Phoungthong, and Makatar Wae-hayee. "Effect Of Equivalent Ratio (ER) On the Flow and Combustion Characteristics in A Typical Underground Coal Gasification (UCG) Cavity." *Journal of Advanced Research in Fluid Mechanics and Thermal Sciences* 86, no. 2 (2021): 28-38. https://doi.org/10.37934/arfmts.86.2.2838

[23] Anderson, John David. *Modern compressible flow: with historical perspective*. Vol. 12. New York: McGraw-Hill, 1990.
[24] Vinayaka, N., C. Akshaya, Avinash Lakshmikanthan, Shiv Pratap Singh Yadav, and R. P. Sindhu. "High Altitude Transonic Aerodynamics of Supercritical Airfoil at different Turbulence Levels." *Journal of Advanced Research in Fluid Mechanics and Thermal Sciences* 60, no. 2 (2019): 283-295.
[25] Fluent, A. N. S. Y. S. "ANSYS fluent theory guide 15.0." *ANSYS, Canonsburg, PA* 33 (2013).
[26] White, Frank M. "Fluid mechanics". *Tata McGraw-Hill Education*, (1979)